REFERENCE EXTRACTION IN DIFFERENCE SPACE FOR MULTIVARIATE IMAGE ANALYSIS

Billaud Eliot, Richard Noël, Fernandez-Maloigne Christine, Rahma Jaber

University of Poitiers, XLIM Laboratory

ABSTRACT

In order to develop a metrological analysis of multivariate images (spectral, multimodal ...) and to reduce the dimensionality of the measures, we propose working in a difference space. The feature space is constructed from the differences between multivariate references and the acquired multivariate measures. This work is focused on automatic reference selection using an iterative extraction process that maximizes the entropy of the total differences. The entropy converges toward a maximum relative to the maximal number of references required to explain the measure data set. Results are developed for a multivariate medical image dataset (MRI).

1. INTRODUCTION

According to our expected metrological properties, we require multivariate image analysis solutions independent from the imaging sensor. Rather than working in the acquisition space (sensor dependent), the analysis is translated into difference spaces relative to multivariate references (reference dependent) [1]. The translation is developed with the hypothesis that the spectral or multivariate distance between a given sample and a reference is preserved regardless of the spectral resolution or the modality count (for compatible spectral range) [2, 3]. The remaining question we develop in this work is about the automatic selection of the spectral or multivariate references.

In the following we will develop automatic reference selection maximizing the total entropy of the obtained difference space. Then we will analyze the obtained difference space and its use in a classification context. The application context is developed for MRI images, a particular case of multivariate images. Even if the medical context is far from remote sensing, the expectations are the same : improve accuracy, reduce uncertainties, take care of the rich information provided by the multivariate sensor.

2. REFERENCE EXTRACTION FOR MULTIVARIATE IMAGES

The analysis of multivariate, multispectral and hyperspectral images raises the issue of the complexity arising from the dimensionality of these images. Most approaches rely on a direct reduction of this dimensionality using various techniques, such as PCA[4], ICA[5], f-PCA[6] or NMF [7].

Only the f-PCA approach preserves some of the physical properties of the measured spectra, as standard operations such as addition, multiplication by a constant and subtraction cannot be applied to reflectance measurements. Another problem with approaches such as PCA, ICA and NMF-type is that they implicitly treat multivariate measurements as vectors, which is not suitable for spectra or multimodal measurements.

3. THE PROPOSED APPROACH

Translating the multivariate analysis of spectral or multimodal images into difference spaces is equivalent to dimension reduction. The expected goal in this case is not to find a feature space minimizing a cost function, but to find a representation improving the cluster identification. The selected optimization criterion is then the total entropy processed in the difference space.

Be I, a multivariate image associating to each p spatial location n measures defined positively by nature : $I(p) \mapsto \mathbb{R}^{+n}$. This measure space is associated with a distance or similarity measure $d() : d\big(I(p), I(q)\big) \in \mathbb{R}^{+}$. Considering S_i, the multivariate measures in $I(p)$ with $0 \leq i < N_{\mathcal{S}}$ and Ref_j 1 of the selected references (same dimensions as $I(p)$). We can define the set of joint differences $\mathcal{D}$ between the set of multivariate measures $\mathcal{S} = \{S_0, S_1 \ldots, S_{N_{\mathcal{S}}-1}\}$ to the selected references $\mathcal{R} = \{R_0, R_1 \ldots, R_{N_{ref}-1}\}$. In this study, the selected references are owned by the initial dataset, so the multivariate image or the set of multivariate images, so $\mathcal{R} \subset \mathcal{S}$.

Considering the joint differences $\mathcal{S}$ as discrete random variables, with values related to the prob-

ability $p_i = prob\big(i \cdot \delta \leq d_i < i \cdot \delta + 1\big)$ and δ corresponding to the bin size. The Shannon entropy is classically defined by:

$$H(D) = \sum p_i \log\left(\frac{1}{p_i}\right) \tag{1}$$

The more relevant reference, R_0, for the set of multivariate measures $\mathcal{S}$ is then defined as maximizing the entropy in the difference set:

$$R_0 = \underset{S_i \subset \mathcal{S}}{\operatorname{argmax}}\, H\Big(d(\mathcal{S}, S_i)\Big) \tag{2}$$

The other references are iteratively extracted, constructing a table of joint differences, including the previously extracted references:

$$R_{k+1} = \underset{S_i \subset \mathcal{S}}{\operatorname{argmax}}\, H\left(d(\mathcal{S}, S_i) \bigcap \left(\bigcap_{j:0 \mapsto k} d(\mathcal{S}, R_j)\right)\right) \tag{3}$$

4. RESULTS AND DISCUSSIONS

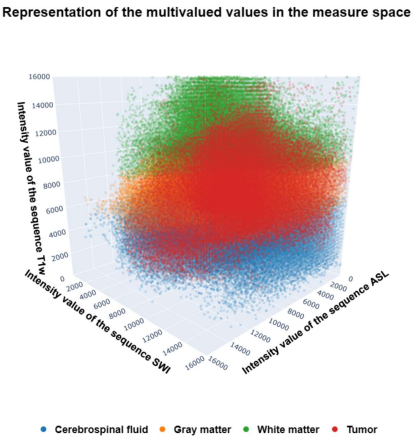
For the experimental part, we chosen to develop it for MRI images. These images are similar to multispectral images: from 1 to 14 modalities can be considered and the different modalities are not orthogonal. In addition, the pixel or voxel measure is a mixing between several kinds of tissues. But mainly, the radiologist community expressed the requirement for metrological solutions [8]. So we are trying to adapt our metrological solutions for remote sensing to the expectations of medical imaging.

Our experimentation is based on the public UCSF-PDGM dataset, version 5 ([9]), which contains 501 cases of tumor-affected brains, each with 14 modalities from different MRI examinations. This allows us to process each case in a multivariate context, comparable to a spectral approach.

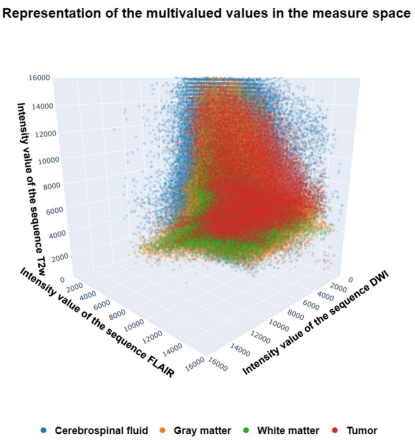
In our experimentation, we used a subset of 20 cases, selected based on common criteria available in the dataset metadata (”WHO CNS Grade”: 2 — ”Final pathologic diagnosis”: Astrocytoma, IDH-mutant — ”IDH”: IDH1 p.R132H). Each case includes 8 modalities (ADC, ASL, DWI, FLAIR, SWI, T1c, T1w, T2w) and a brain segmentation into 4 classes (cerebrospinal fluid, gray matter, white matter, tumor).

All modalities were normalized using a histogram matching to a reference model (one model per modality), combined with a double interpolation to preserve fine details (texture). As a result, all brain acquisitions share the same dynamic range (as shown in Figure 1).

In Figure 2, the entropy evolution according to the extracted reference count is presented. As expected, the entropy grows up with the first reference extractions before to saturate. For the first four references, adding one reference allows to observe new clusters in the difference space. After the fourth reference, adding reference doesn't allow observing new clusters inducing the saturation of the entropy. So only four references are sufficient to capture the whole complexity of the multivariate dataset. The reference locations in 3 of the 8 modalities are displayed in



(a) ASL, SWI, and T1w modalities



(b) DWI, FLAIR, and T2w modalities

Fig. 1: Representation of the multivariate data in the measure space.

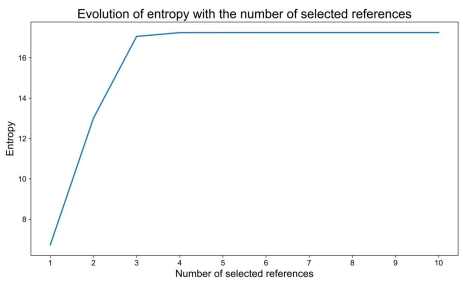


Fig. 2: Entropy evolution relative to the number of selected references.

Figure 3, as expected from [2]. They are founded on the convex hull framing the dataset. They are well distributed in the measured space, allowing so to explore the multivariate diversity. Figure 4 shows some multivariate responses of the different classes and the 4 extracted references. It illustrates the difficulty of the classification, all the multivariate responses have similar dynamics induced in part by the normalization, and the variations are mainly in the multivariate shape of the multimodal signals. As expected, the 4 extracted references are not similar to the multimodal samples, as they are selected at the border of the data hull, so far from the center of the measure set.

In order to illustrate the use of the multivariate difference space in decision-making, we propose to apply a classification scheme to the obtained differences. The inner difference used in this case is an order-2 Minkowski metric (L_2) and the classification approach is based on the SVM approach.

Unfortunately, the obtained results in the difference space are lower than those directly obtained in the measure space. Two main reasons can explain this limit and define the next trends. Firstly the nature of the difference space is based on distance to reference.

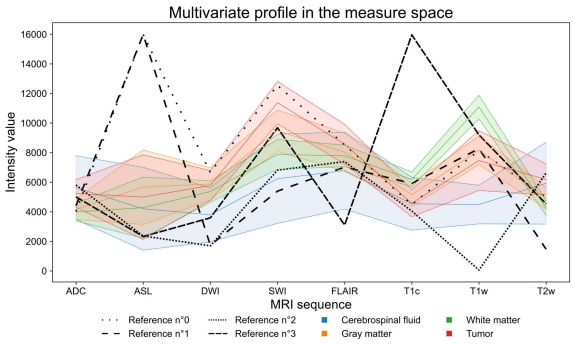
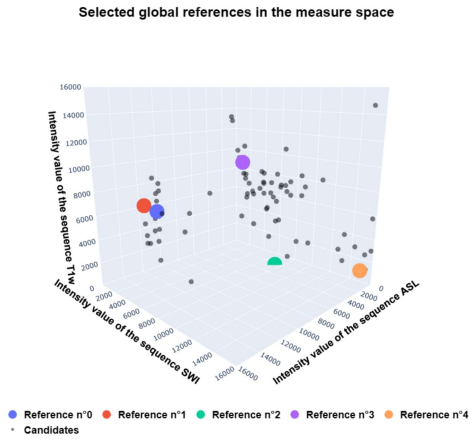
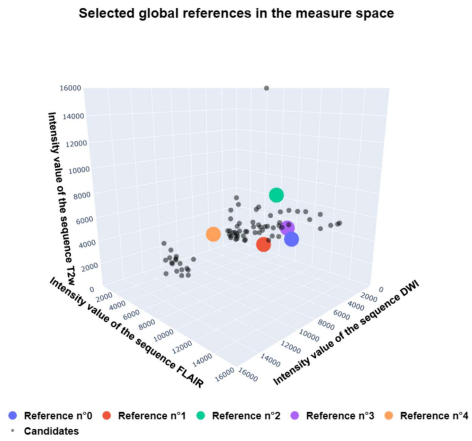


Fig. 4: Extracted multivariate average (colored lines) and standard deviation for each segmentation class across the dataset. Black discontinued lines represent the 4 selected references extracted from the dataset.

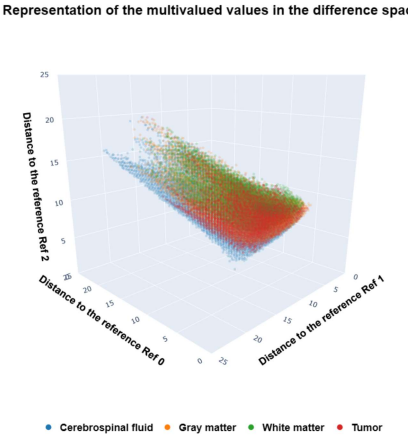


(a)ASL, SWI, and T1w modalities

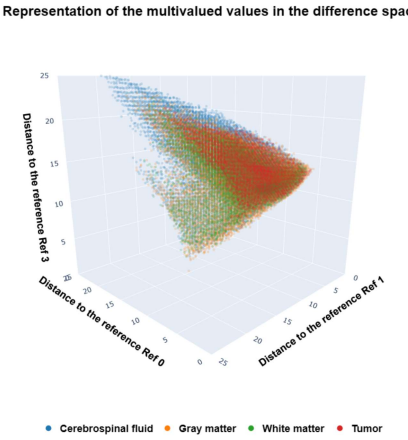


(b) DWI, FLAIR, and T2w modalities

Fig. 3: Local references extracted from each subject (black dots) and global references selected from them (colour dots) in the measure space.



(a) References 0, 1 and 2



(b) References 0, 1 and 3

Fig. 5: Representation of the multivariate MRI data in the difference space relative to the 4 global references.

	Acc.	Prec.	Rec.	F1.
Measure space	0.83	0.74	0.73	0.73
Difference space	0.78	0.65	0.68	0.66

Table 1: Performance criteria of the SVM classification in the different spaces

	1	2	3	4
1	0.8	0.17	0.01	0.02
2	0.06	0.8	0.11	0.03
3	0.0	0.05	0.94	0.0
4	0.12	0.4	0.07	0.4

(a) Classification in the measure space

	1	2	3	4
1	0.73	0.18	0.05	0.04
2	0.08	0.72	0.12	0.08
3	0.01	0.06	0.93	0.
4	0.29	0.31	0.08	0.33

(b) Classification in the difference space

Table 2: Confusion matrices of the SVM classification in the different spaces

By nature the difference in space is a metric space, so with measures defined positive, and in the case of $L2$ metrics following a quadratic law. The linear SVM is not adapted to this feature space. To take care of this construction, an adapted homeomorphism must be defined to construct a feature space facilitating the classification.

The second reason is explained by the Figure 4. MRI domain is not usual with multivariate image analysis, and in the selection of the adapted multivariate distance. Using $L2$ metrics and the derivative as Mahalanobis distance is the norm, so at the core of the scientific path constructed in this work. Considering the Figure 4, we can observe that the multivariate class responses are more different in the shape structure than in the global intensity variations, so distance or similarity metrics are based on shape differences, like Spectral Angle Mapper, Spectral Information Divergence or Kullback-Leibler pseudo divergence would be more adapted for discrimination purposes.

5. CONCLUSION

In this work, we presented, for the first time, the automatic selection of references for difference-based feature spaces. This approach is generic and initially developed for multi and hyperspectral image analysis. It is based on a reference selection from the initial dataset, using a criterion based on the entropy calculated in the difference space. In this work, we selected to illustrate its use on a particular domain of multivariate images, which are the MRI images. Twenty 3D MRI images acquired on 8 modalities were used in a classification approach (4 classes). The results show that MRI images require dedicated difference measures coming from the remote sensing domain as spectral shape differences (SAM, SID, KLPD ...). Finally, it is important to note that very few voxels are 'pure'; in reality, almost all of them contain a mixture of several types of tissue (white matter, gray matter, ...), which makes it necessary to use unmixing methods for voxel characterization.

6. REFERENCES

[1] H. Deborah et al., "16 - metrological hyperspectral image analysis through spectral differences," in *Hyperspectral Remote Sensing*, Earth Observation, pp. 319–340. Elsevier, 2020.

[2] Noël Richard et al., "Pseudo-divergence and bidimensional histogram of spectral differences for hyperspectral image processing," *Journal of Imaging Science and Technology*, vol. 60, no. 5, pp. 50402–1–50402–13, 2016.

[3] H. Deborah et al., "A comprehensive evaluation of spectral distance functions and metrics for hyperspectral image processing," *IEEE J. Sel. Topics Appl. Earth Observ. Remote Sens.*, vol. 8, no. 6, pp. 3224–3234, 2015.

[4] H. A. Khan et al., "Hytexila: High resolution visible and near infrared hyperspectral texture images," *Sensors*, vol. 18, no. 7, 2018.

[5] Jing Wang et al., "Independent component analysis-based dimensionality reduction with applications in hyperspectral image analysis," *Geoscience and Remote Sensing, IEEE Transactions on*, vol. 44, pp. 1586 – 1600, 07 2006.

[6] Yantao Wei et al., "Hyperspectral image classification using fpca-based kernel extreme learning machine," *Optik*, vol. 126, no. 23, pp. 3942–3948, 2015.

[7] Lei Zhou et al., "Subspace structure regularized nonnegative matrix factorization for hyperspectral unmixing," *IEEE Journal of Selected Topics in Applied Earth Observations and Remote Sensing*, vol. 13, pp. 4257–4270, 2020.

[8] Daniel C. Sullivan et al., "Metrology standards for quantitative imaging biomarkers," *Radiology*, vol. 277, no. 3, pp. 813–825, 2015.

[9] Evan Calabrese et al., "The University of California San Francisco Preoperative Diffuse Glioma MRI Dataset," *Radiology: Artificial Intelligence*, vol. 4, no. 6, pp. e220058, Oct. 2022.